방사선방어학회지
제12권 제1호 1987

論 文

Central Axis Percentage Depth-Dose in a Water Phantom Irradiated by Conventional X-rays

Wuôn-Shik Kim, Suck-Ho Hah, Sun-Tae Hwang

Radiation Laboratory, Korea Standards Research Institute, Taejon, Korea

Jang-Jin Oh and Jae-Shik Jun

Department of Physics, Chungnam National University, Taejon, Korea

=Abstract=

Central axis percentage depth-doses, P(%), were measured at the points from the 2.5 cm depth of reference point to 20 cm depth with 2.5 cm interval. Distance from the X-ray target to the water phantom ($30\times30\times30$ cm^3) surface was 1 m, and at this point three different beam sizes of 5cmϕ, 10 cmϕ and 15 cmϕ were used. While the X-ray tube voltage varied from 150 to 250 kV, the tube current remained constant at 5 mA. Absorbed dose rate in water, $\dot{D}_w$, was determined using the air kerma calibration factor, N_k, which was derived from the exposure calibration factor, N_x, of the NE 2571 ion chamber. The reference exposure rate, $\dot{X}_c$, was measured using the Exradin A-2 ion chamber calibrated at ETL, Japan. The half value layers of the X-rays determined to meet ETL calibration qualities.

The absorbed dose rates determined at the calibration point were compared to the values obtained from Burlin's general cavity theory, and the percentage depth-dose values determined from N_k showed a good agreement with the values of the published depth dose data (BJR Suppl. 17).

I. INTRODUCTION

The ultimate aim of clinical radiation dosimetry is to determine the absorbed dose completely, i.e., three dimensional distribution in a water phantom thence in the patient.

For this purpose four stages are usually involved. First, a determination of the radiation is made at the calibration point. Such a determination is required for all beam sizes and source distances that are to be used. Secondly, the peak absorbed dose rates or, for low energies (below 400 kV of tube voltage), the surface absorbed dose rates are deduced either by relative measurements or, more usually, with the aid of published depth-dose tables. In the third stage, the absorbed dose rate at any point of interest is related to the peak or surface absorbed dose rate by the use of appropriate standard depth-dose tables and isodose charts. Finally, correction may have to be made for the fact that the shape, size and composition of the patient are different from those of the pha-

ntom in which the standard measurements were made. An essential step to this process is to establish the variation in absorbed dose along a single ray, and the most useful one is the central ray.

In this paper, we tried to establish the percentage depth-dose tables for sentral X-arys having 0.88 mmCu, 1.68 mmCu and 2.60 mmCu HVL. And the X-ray target to phantom surface distance(SSD) was 100 cm constant. Absorbed dose was measured with ionization method. The theories for the absorbed dose determination and for the evaluation of percentage depth-dose are given in section Ⅱ. The experimental method of the measurement of absorbed dose in water and of X-ray qualities are discussed in section Ⅲ. In section Ⅳ, the exposure calibration factor, N_x, the air kerma calibration factor, N_k, the absorbed dose rate in water, $\dot{D}_w$, and the percentage depth dose, P(%), are determined. Then, $\dot{D}_w$ values determined from N_k were compared with the values calculated from the Burlin's general cavity theory. The P(%) values determined were compared with the published depth dose data. The conclusion follows in section V.

II. THEORY

The exposure is defined as X=dQ/dm, where dQ is the charge produced in air by the secondary electrons ejected by photons in a mass dm of air. If the mean energy required to produce an ion pair in air is W, then the imparted energy per unit mass of air, i.e., the absored dose in air, is

$$D_{air}=dE\left(\frac{dE}{dm}\right)_{air}=\frac{dQ\cdot W/e}{dm}=X\cdot\frac{W}{e}$$

under condition of electron equilibrium. Thus from mass energy absorption coefficient ratio, the absorbed dose to material m is

$$D_m=X\cdot\frac{W}{e}\cdot\left(\frac{\mu_{en}}{\rho}\right)_{m,air} \quad \cdots(1)$$

where $(\mu_{en}/\rho)_{m,air}$ is $(\mu_{en}/\rho)_m/(\mu_{en}/\rho)_{air}$. From Bragg-Gray equation, the absorbed dose in material m which is surrounding the air cavity becomes

$$D_m=S_{m,air}\cdot J\cdot W/e \quad \cdots(2)$$

where $S_{m,air}=(S/\rho)_m/(S/\rho)_{air}$, and J is the charge per unit mass of the air cavity resulting from ionization produced by the electrons. Then, from eqs. (1) and (2), the exposure becomes

$$X=J\cdot S_{m,air}\cdot(\mu_{en}/\rho)_{air,m} \quad \cdots(3)$$

Using energy fluence, Ψ, the exposure, X, and the air kerma, K_{air}, are related as follows:

$$X=\Psi\cdot\left(\frac{\mu_{en}}{\rho}\right)_{air}\cdot\frac{e}{W}$$

$$K_{air}=\Psi\cdot\left(\frac{\mu_{tr}}{\rho}\right)_{air}=X\cdot\frac{W}{e}\cdot\left(\frac{\mu_{tr}/\rho}{\mu_{en}/\rho}\right)_{air}$$

$$=\frac{X\cdot W/e}{1-g_B}\approx(1+g_B)\cdot\frac{W}{e}\cdot$$

$$[S_{m,air}\cdot(\mu_{en}/\rho)_{air,m}]\cdot J \quad \cdots(4)$$

where g_B is the fraction of electron energy lost in bremsstrahlung productron, and $(\mu_{en}/\rho)_{air}$ and $(\mu_{tr}/\rho)_{air}$ are the mass energy absorption and mass energy transfer coefficient of air, respectively.

1. Determination of Absored Dose via Air Kerma Calibration Factor

In case that the of exposure standards have been established, N_k is recalculated from N_x and eq. (4) as follows[1]

$$N_x=\frac{X_c}{M} \quad \cdots(5)$$

$$N_k=\frac{K_{air,c}}{M}=\frac{X_c\cdot W/e}{M(1-g_B)}$$

$$=N_k\cdot\frac{W}{e}\cdot\frac{1}{1-g_B} \quad \cdots(6)$$

where the meter reading of the ion chamber M, reference exposure X_c and reference air kerma $K_{air,c}$ are determined in calibration

quality field. The water kerma, K_w, is then obtained from

$$\frac{K_w}{K_{air}}=\left(\frac{\mu_{tr}}{\rho}\right)_{w,air} \quad \cdots(7)$$

where $(\mu_{tr}/\rho)_{w,air}$ is (μ_{tr}/ρ) water/$(\mu_{tr}/\rho)_{air}$. In the conventional X-ray energy region, $g_B \approx 0$ and therefore $(\mu_{tr}/\rho)\approx(\mu_{en}/\rho)$, and furthermore

$$D_w=K_w(1-g_B)\approx K_w$$

Thus from eqs. (6) and (7)

$$D_w\approx M_u\cdot N_k\cdot k_u\left(\frac{\mu_{en}}{\rho}\right)_{w,air}\cdot P_u \quad \cdots(8)$$

where P_u is the perturbation correction factor for the replacement of water by air, and $M_u=M_u^0\cdot P_{tph}\cdot P_s$, where M_u^0 is the meter reading in water phantom, P_{tph} is the factor for temperature, pressure and humidity correction, and P_s is the factor for lack of saturation charge correctively. In addition k_u is a factor to accomodate the possible difference in sesitivities of N_k between the calibration and the user fields of radiation.

2. Determination of Absorbed Dose via Burlin's General Cavity Theory

The purpose of cavity theory is to relate the absorbed dose in a cavity or detector of arbitrary size and composition to the absored dose in the surrounding medium of different atomic number or composition by means of the equation.

$$D_m=\frac{1}{f_{cm}}\cdot D_c \quad \cdots(9)$$

where D_c is the cavity dose, and D_m is the does when the cavity is filled with the surrounding medium material. f_{cm} is in general a function of the X-ray energy, the composition of the cavity and the surrounding medium, and the cavity size.

Burlin proposed an approximate general cavity theory[2,3,4] for photons for all caviy sizes, which approaches the Spencer-Attix theory[5] in the small size limit and reduces the ratio of the mass energy absorption ceofficients for large cavities. In Burlin's general cavity theory, f_{cm} is given by

$$f_{cm}=d\bar{S}_{cm}+(1-d)(\bar{\mu}_{en}/\rho)_{cm}. \quad \cdots(10)$$

If g is the average path length of electrons crossing the cavity, then,

$$d=\int_0^g \exp(-\beta x)\,dx/\int_0^g dx$$
$$=\frac{1-\exp(-\beta g)}{\beta g} \quad \cdots(11)$$

where β is the mass energy fluence attenuation coefficient of the secondary electron. spectrum Many experimental studies have indicated that the exponential attenuation is determined in terms of the maximum elec tron energy, E_{max}. Burlin adopted the formula [2,3,4,6].

$$\beta=16(E_{max}-0.036)^{1.40}(cm^2\cdot g^{-1}),$$
$$g=4\rho V/s(g\cdot cm^{-2}) \quad \cdots(12)$$

where ρ is the air density, V and S are the volume and the total surface area of the dosimeter, respectively.

For the case of cavity size much less than the secondary electron range produced in the walls, the total electron fluence in this cavity is deiermined by both the production and scatter of the secondary electrons from the wall materical. That is, the electron fluence within the cavity is independent of the cavity material. As the cavity size increases, the analysis becomes complicated due to several factors. First, photon interactions with the cavity material are no longer negligible; second, the attenuation of the electron fluence becomes important; and third, the electron scattering properties of the cavity material gradually increase in importance. The first two effects were taken account in the well known Burlin's general cavity the-

ory[2]. Horowitz et al.[6,7] demonstrated that taking the third effect, electron scattering, into account can improve the Burlin's model. And recently, Kearsley[8] suggested new general cavity theory which is the only one capable of yielding cavity dose distributions, but requires further experimental and theoretical development due to the relativey large number of unknown parameters it implies. For moderately mismatched cavity and medium, those three expressions for general cavity theory were compared in detail by Horowitz[4], and all the three expressions give excellent agreement with the experimental data from the landmark Ogunleye et al. Thus, in this study we used Burlin's expression for its greater simplicity.

In the case of the cavity chamber located in water phantom, and the chamber wall and its dosimetry gas composed of graphite and air, respectively, the absorbed dose in water is represented from eqs. (2) and (9) as

$$D_w = D_{g_r} \cdot (\mu_{en}/\rho)_{w,g_r} = \frac{1}{f_{\mathrm{air},g_r}} \cdot D_{\mathrm{air}} \cdot (\mu_{en}/\rho)_{w,g_r} = \frac{1}{f_{\mathrm{air},g_r}} \cdot J \cdot (W/e) \cdot (\mu_{en}/\rho)_{w,g_r} \quad \cdots (13)$$

where D_{g_r} is the absorbed dose in graphite.

3. Determination of the Average Primary Electron Energy $\bar{T}_e$

For conventional X-ray energy region (70 kV to 300 kV), the primary electron produced in the medium may be resulting from the photoelectric interaction or Compton scattering interaction with incident primary photon. In case of photoelectric interaction, the primary electron will have the energy $T_{PE} = h\nu - E_b \approx h\nu$, where $h\nu$ is the incident photon energy, and E_b is the binding energy of the electron in the atom (in solid medium, $E_b \approx 3$ eV). For the Compton scattering interaction, the primary electron will have the energy $T_c = h\nu \cdot \frac{{}_e\sigma_a}{{}_e\sigma}$, where ${}_e\sigma$ is the Compton cross section per electron, and ${}_e\sigma_a$ is the differential cross section of the energy transfer to the recoiled electron. Thus taking single Compton scattering approximation, we have

$$\bar{T}e = h\nu \cdot \frac{A_{PE}}{A_{PE}+A_c} + h\nu \cdot \frac{{}_e\sigma_a}{{}_e\sigma} \cdot \frac{A_c}{A_{PE}+A_c} \quad \cdots (14)$$

where A_{PE} is the photoelectric cross section, and A_c is the Compton scattering cross section for elements or compounds.

4. Determination of the Percentage Depth-Dose

Percentage depth-dose is defined as the ratio (expressed as a percentage) of the absorbed dose at a given depth in a medium to the absorbed dose at a fixed reference point on the beam axis. In clinical work it is customary to state, for each beam size and shape used, the absorbed dose rate at the reference point of the central percentage depth dose values, that is, at the point at which the value of the percentage dose is 100. For radiations generated by potentials below 400 kV, reference point is at the surface, while for higher energy radiations it is at the position of the peak absorbed dose.

Thus, the percentage depth dose, $P(\%)$, as shown in Fig. 1, is defined as[9]

$$P(d,d_0W,S,E_{eff}) = \frac{D_d}{D_{d_0}} \cdot 100(\%) \quad \cdots (15)$$

where D_d and D_{d_0} are the absorbed dose at depth d_0, respectively. d and d_0 are the depth of measurement point and the reference, point respectively, W is the field dimension (When the mode used employ a fixed source to surface distance, the field size is defined

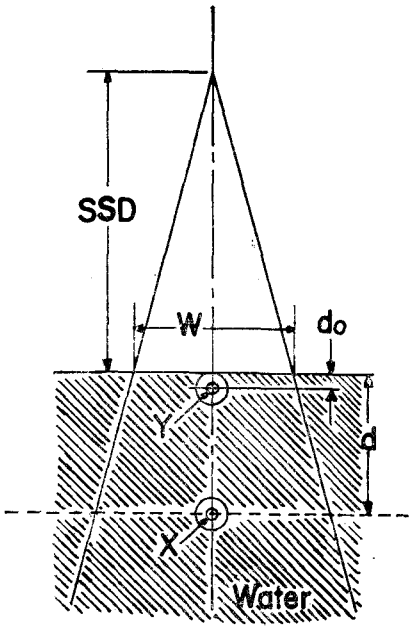

Fig. 1. Schematic diagram illustrating the percentage depth dose.

at surface of the phantom), S is the source to surface distance (=SSD), and E_{eff} is the effective energy or quality of incident radiation.

III. EXPERIMENT

The calorimetry and the ionization method are those of the absolute measurement methods of absorbed dose, but below 1 Gy only the ionization method is applicable[10]. Thus the latter one was used in our study.

At first, the reference exposure rate was determined at the position 1 m away from the X-ray target using Keithley 616 electrometer with 6169 Digital interface and Exradin 3.6 cc A-2 ionization chamber which had been calibrated at ETL, Japan, to meet the international radiation traceability. The radiation quality of an X-ray beam in practical use is normally characterized by the tube voltage, total filtration and first half value

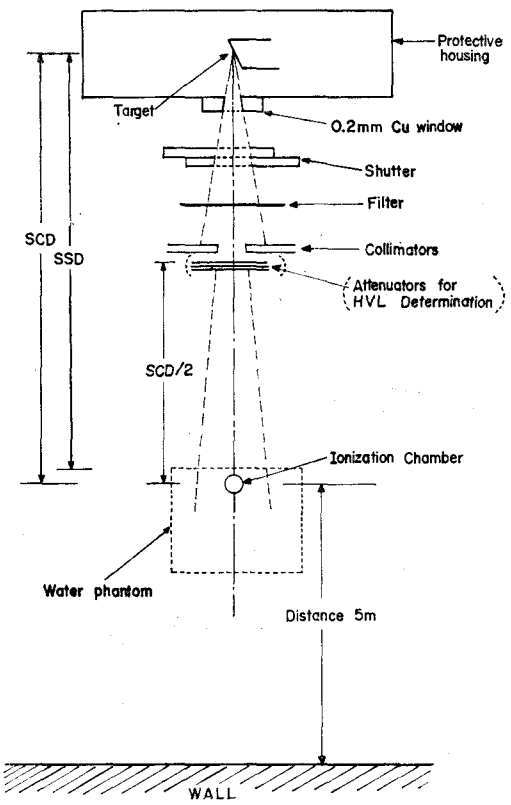

Fig. 2. Schematic diagram of KSRI 300 kV level X-ray calibration system.

layer. Thus, the first half value layers of the KSRI 300 kV level X-ray calibration system were determined as to ETL calibration quality. Then, to check the X-ray qualities determined from HVL method and their changes in the water phantom, the X-ray energy spectra with and without penetrating the water phantom were measured using a high purity Ge detector and a 8192 channel multi-channel analyzer.

Fig. 2 illustrates the KSRI 300 kV X-ray system. In order to line up X-ray to 4 m rail system, we used the radiography method employing the central ray of the laser[11].

Then, the values of N_x and N_k of the NE 0.6 cc 2571 ion chamber were determined via

Table 1. KSRI X-ray qualities(Tube current: 5 mA, SCD: 100 cm, Beam size: 5 cmϕ)

Code of X-ray quality	Tube voltage (kV)	Total filter		1 st HVL (mm)	Eeff(keV)
		Inherent (mm)	Added(mm)		
KS-X0150	150	0.20 Cu	0.76 Cu+0.31 Al	0.88 Cu	76
KS-X0200	200	0.20 Cu	1.5 Cu+0.1 Al	1.68 Cu	100
KS-X0250	250	0.20 Cu	2.25 Cu+0.21 Al	2.60 Cu	125

Table 2. Determined values of $\bar{T}e$(keV), $\bar{S}/\rho$(MeV. cm^2/g) and $(\mu_{en}/\rho)_{air,m}$

Material / Item / Code of X-ray	Air			Graphite			Water		
	$\bar{T}e$	$\bar{S}/\rho$	$(\mu_{en}/\rho)_{air,m}$	$\bar{T}e$	$\bar{S}/\rho$	$(\mu_{en}/\rho)_{air,m}$	$\bar{T}e$	$\bar{S}/\rho$	$(\mu_{en}/\rho)_{air,m}$
KS-X0150	11.50	17.71	1	9.69	20.66	1.2175	11.21	20.62	0.9312
KS-X0200	15.48	14.02	1	14.42	15.15	1.0821	15.27	16.23	0.9135
KS-X0250	21.28	11.05	1	20.57	11.53	1.0331	21.11	12.65	0.9045

the reference exposure rate. using this N_k, $\dot{D}_w$ was determined in the water phantom at the points from 2.5 cm depth, reference point, to 20 cm depth with 2.5 cm interval. From this result, the percentage depth dose was determined. The overall thicknses of the lucite$(C_5H_8O_2)_n$ phantom wall is 10 mm, but it is 4 mm or less at the beam entrance and exit portion.

In this experiment, SSD 1 m, and at this position beam sizes were 5, 10 and 15 cmϕ. While X-ray tube voltages were varied from 150 to 250 kV, tube current remained constant at 5 mA.

IV. RESULTS AND DISCUSSION

1. Determination of the X-ray Qualities

First half value layers were Qetermined using Al and Cu filters of 99.9% purity having 10×10 cm^2 size, and they are summarized in Table 1.

On the other hand, the effective energies of the X-rays measured by x-ray spectrometry method were 79.9 keV and 127.7 keV for tube voltages of 150 kV, 200 kV, respectively[11].

The X-ray spectrum change in the water phantom was turned out negligible compared to its effective energy.

Table 3. Exposure calibration factor, N_x, and air kerma calibration factor, N_k, of NE 2571 in chamber

Item / Code of X-ray	$N_x(\times10^6 kg^{-1})$	$N_k(\times10^7 G_y C^{-1})$
KS-X0150	1.137	3.862
KS-X0200	1.125	3.822
KS-X0250	1.119	3.801

2. Comparison of D_w Values Determined via N_k and Burlin's General Cavity Theory

$\bar{T}_e$ was calculated from eq(14), and required coefficients of $_e\sigma_a$ and $_e\sigma$ were referred to F.H. Attix and W.C. Roesch[2], A_{PE} and A_c were referred to J.H. Hubbel[12]. From this calculated values of $\bar{T}_e$, the average mass stopping power, $\bar{S}/\rho$, of the related materials was determined from ICRU Report 37[13]. The

Table 4. $\beta(cm^2, g^{-1})$, $g(g \cdot cm^{-2})$, d and $f_{air,gr}$ in Burlin's general cavity theory

Item / Code of X-ray	β	g	d	$f_{air,gr}$
KS-X0150	1,747.50	6.982×10^{-4}	0.5780	1.0093
KS-X0200	925.99	6.982×10^{-4}	0.7364	0.9667
KS-X0250	596.76	6.982×10^{-4}	0.8178	0.9719

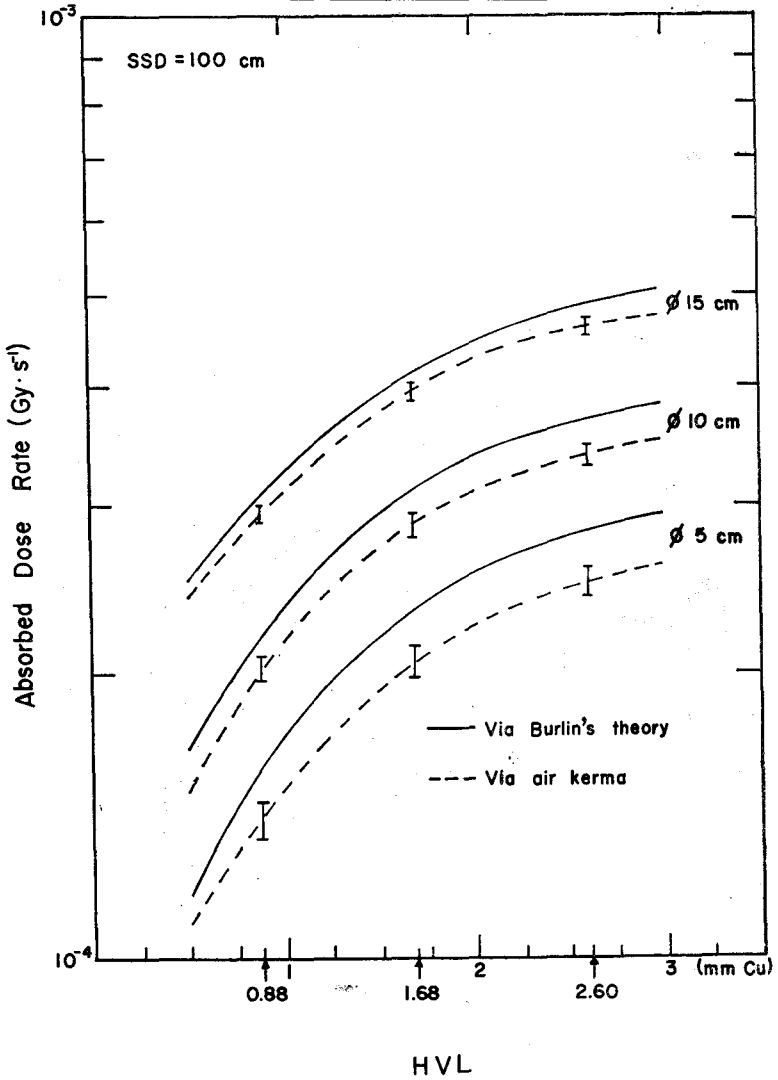

Fig. 3. Comparison of the $\dot{D}_w$ values, at the calibration point of 5 cm depth, determined via N_k(solid curve) and Burlin's general cavity theory(broken curve).

average mass energy absorption coefficient ratio of material to air, $(\mu_{en}/\rho)_{m,air}$, was determined using J.H. Hubbel's data[14] for incident photon energies. In conventional X-ray energy, the required electron energy to cross just the cavity, denoted by $\triangle$, is about 10 keV. Hence, the difference between restricted stopping power and stopping power is negligible for air, graphite and water[13]. The values of $\bar{T}e$, $\bar{S}/\rho$ and μ_{en}/ρ are given in

Table 2.

Values of N_x and N_k of NE 2571 ion chamber determined from the values of X_c, eqs. (5) and (6) are summarized in Table 3. In this study we used the values of 33.97 J/c for W/e and 0.94×10^{-4} for g_B[13]. Using the values of Tables 2 and 3, the absorbed dose rate in water at the calibration point was calculated from eq. (8), and described in Fig. 3 in solid curve. In this calculation the photon energy spectrum change in the water phantom was negligible, compared to its effective energy k_u was taken to be equal to 1.0, and P_u was taken as 1.05, 1.03 and 1.02 for tube voltage 150 kV, 200 kV and 250 kV, respectively[15].

The calculated values of β, g, d f_{air,g_r} are summarized in Table 4. Using eq. (13), Tables 2 and 4, the absorbed dose rate in water at the calibration point was calculated via Burlin's general cavity theory. This result is described in Fig. 3 in broken curve.

3. Comparison of P(%) Values Determined via Our Experiment and that via Published Depth Dose Data.

From eq. (8), Tables 2 and 3, the absorbed dose rates at the points from 2.5 to 20 cm depth on the central ray in the water phantom were determined. Using these results, the percentage depth dose was determined from eq. (15), and listed in Table 5. The total uncertainty in the depth range 2.5 to 10 cm is less than $\pm3\%$, in the range 10 to 15 cm it is less than $\pm4\%$ and in the range 15 to 20 cm, less than $\pm5\%$. The increasing uncertainty is seems to be due to the dependence of small ionization current with depth.

Also, the percentage depth dose data are available for HVL of the range from 0.5 to

Table 5. Comparison of the P(%) values measured from our experiment and obtained for BJR Suppl. 17(SSD: 100 cm, Reference depth d_0 : 2.5 cm)

Code of X-ray	KS-X0150						KS-X0200						KS-X0250					
Beam dia. (cm)	5		10		15		5		10		15		5		10		15	
Depth(cm)	Exp.	Pub.	Exp.	Pub.	Exp.	Pub.	Exp.	Pub.	Exp.	Pub.	Exp.	Pub.	Exp.	Pub.	Exp.	Pub.	Exp.	Pub.
2.5	100	100	100	100	100	100	100	100	100	100	100	100	100	100	100	100	100	100
5	67.6	69.0	75.7	74.9	80.9	79.8	71.3	69.8	76.9	76.8	82.2	81.5	71.6	69.8	77.3	77.2	82.9	81.8
7.5	45.3	—	52.5	—	59.4	—	47.9	—	43	—	63.5	—	49.3	—	58.4	—	64.1	—
10	29.0	29.3	35.7	36.7	43.0	41.5	32.0	32.2	38.5	39.7	47.2	46.1	32.5	33.3	41.8	41.0	47.6	46.8
12.5	18.5	—	24.3	—	30.1	—	21.1	—	27.6	—	33.5	—	22.8	—	28.9	—	34.8	—
15	11.4	12.8	15.9	17.6	20.8	21.2	13.8	14.2	18.7	20.2	24.1	24.1	15.5	15.6	20.9	21.3	25.4	25.6
17.5	7.8	—	11.0	—	14.0	—	9.4	—	12.8	—	16.6	—	10.2	—	14.4	—	18.5	—
20	4.9	—	17.2	—	9.6	—	6.6	—	8.9	—	11.9	—	6.9	—	10.1	—	13.2	—

3.0 mmCu (diaphragm limited square field, SSD=50cm)[16].

Conversion factors of equivalent square field to circular field (by M.J. Day et al.) and P(%) values of one SSD to another (J.E. Burns et al.) are available from the appendix of BJR Suppl. 17. Using this published depth dose data, the P(%) values under similar condition to ours can be determined. The differences between P(%) determined from our experiment and BJR Suppl. 17 are within 8 percents. On the other hand R.M. Harrison[17] had measured P(%) for X-rays having 1.0 to 4.0 mmAl HVL at the point from 0 to 16 cm in depth with 60 cm SSD. His results are different by 10 percents or less from the values of BJR Suppl. 11. These differences seem to be due to the inadequacy of the first HVL as the sole specifier of beam quality, i.e., those peak tube voltages in BJR Suppl. 11 and 17 are not the same as Harrison's and ours, respectively.

The percentage depth dose determined from our experiment and from BJR Suppl. 17 are compared in Table 5.

V. CONCLUSIONS

The following conclusions are derived from this study.

1. The exposure calibration factor, N_x ($\times 10^6 kg^{-1}$), is ranged from 1.119 to 1.137 and the air kerma calibration factor, N_k($\times 10^7$ $Gy.C^{-1}$), is from 3.801 to 3.862 for the NE 0.6 cc 2571 ionization chamber.

2. The weighting factor, d, in Burlin's general cavity theory is turned out to be from 0.578 to 0.818. This means that in case of electron range in air cavity is comparable to the cavity size, the contribution of direct photon interaction with cavity itse lf is not negligible. But, with the photon energy is increasing, the chamber wall contribution is more dominent than that of the air cavity. Since graphite wall is air equivalent material, $f_{air,g_r} \rightarrow 1$ as it should.

3. The absorbed dose rate in water, $\dot{D}_w$, and the percentage depth-dose, P(%), determined in the water phantom from 2.5 to 20cm depth with 100 cm SSD are varied from 5.846×10^{-4} to 1.007×10^{-5} ($Gy.s^{-1}$) and from 100 to 4.9, respectively.

4. At the calibration point, the differences between $\dot{D}_w$ evaluated from the N_k and that from the Burlin's general cavity theory amount to 13 percents. This significant difference seems largely due to the error involved in determination of β and g in using Burlin's theory. The choice of eq. (12) assumes that the electrons impinging on the cavity are in a state of quasi-diffusion, furthermore $g=4\rho v/s$ is correct only for isotropically incident radiation and convex cavities. As beam size is increasing from 5 to 15 cmϕ at 1 m from the X-ray target, the difference of the absorbed dose rates determined via N_k and that via Burlin's theory is reduced from 13 to 5.1%.

Thus the determination of β and g should be thoroughly studied in the collimated beam conditions. On the other hand the differences between P(%) (from 2.5 to 20 cm in depth) determined from present experiment and that from BJR, Suppl. 17 are within 8 percents.

REFERENCES

1) Colin G. Orton, *Radiation Dosimetry*, Plenum Press, New York (1986).

2) F.H. Attix and W.C. Roesch, *Radiation Dosimetry*, Vol. 1, 2nd ed., Academic Press, New York (1968).

3) 황선태, 박내웅, 하석호 : "공동전리함이론", KS-

RI-SP-2, 한국표준연구소 (1982).

4) Y.S. Horowitz, "Photon general cavity theory," *Radiat. Protec. Dosim.*, **9**(1), 5-18 (1984).

5) L.V. Spencer and F.H. Attix, "A Theory of cavity ionization," *Radiat. Res.*, **3**, 239-254 (1954).

6) Y.S. Horowitz and A. Dubi, "A proposed modification of Burlin's general cavity theory for photons," *Phys. Med. Biol.*, **27**(6), 867-870 (1982).

7) Y.S. Horowitz, M. Moscovitch and A. Dubi, "Modified general cavity theory applied to the calculation of gamma dose in ^{60}Co thermoluminescence dosimetry," *Phys. Med. Biol.*, **28**(7), 829-840(1983).

8) E. Kearsley, "A new general cavity theory," *Phys. Med. Biol.*, **29**(10), 1179-1187 (1984).

9) International Commission on Radiation Units and Measurements, *Measurement of Absorbed Dose in a Phantom Irradiated by a Single Beam of X or Gamma Rays*, ICRU Report 23 (1973).

10) J.R. Greening, *Fundamentals of Radiation Dosimetry*, 2 nd ed., Medical Physics Handbooks 15(1985).

11) 황선태, 하석호, 김원식, 김현문 : "중경 X선 흡수선량 측정표준", KSRI-87-8-IR, 한국표준연구소 (1987).

12) J.H. Hubbel, "Photon cross sections, attenuation coefficients and energy absorption coefficients from 10 keV to 100 GeV," NSRDS-NBS 29(1969).

13) International Commission on Raiation Units and Measurement, *Stopping Powers for Electrons and Positrons*, ICRU Report 37(1984).

14) J.H. Hubbel, "Photon mass attenuation and energy-absorption coefficients from 1 keV to 20 MeV," *Int. J. Appl. Radiat. Isot.*, **33**, 1269-1290(1982).

15) P. Andreo, A. Nahum and A. Brahme, "Chamber-dependent wall correction factors in dosimetry," *Phys. Med. Biol.*, **31**(11), 1189-1199 (1986).

16) D.K. Bewley, A.L. Bradshaw, D. Greene, J.L. Haybittle and L.F. Secretan, "Central axis depth dose data for use in radiotherapy," *Brit. J. Radiol., Suppl.* **17** (1983).

17) R.M. Harrison, "Central-axis depth-dose data for diagnostic radiology," *Phys. Med. Biol.*, **26**(4), 657-670(1981).

Water Phantom 속 Conventional X-ray 중심축상의 깊이 선량 백분율

김원식 · 하석호 · 황선태

한국표준연구소 방사선연구실

오 장 진 · 전 재 식

충남대학교 자연과학대학 물리학과

=요 약=

X-선 target으로 부터 water phantom(30×30×30 cm^3) 표면까지 1 m이고 이 지점에서 비임 크기가 5 cmϕ, 10 cmϕ, 15 cmϕ인 경우 phantom 표면으로 부터 X-선 중심축을 따라 깊이 2.5 cm의 기준점으로 부터깊이 20 cm까지 2.5 cm 간격으로 깊이—선량 백분율, P(%)을 측정하였다. 사용된 X-선 인가전압 및 전류는 150~250 kV 및 5 mA이었고 물속 흡수선량률, $\dot{D}_w$은 NE 2571 공동전리함의 조사선량 교정인자 N_x로부터 구한 공기 kerma 교정인자 N_k를 이용하여 결정하였다. 기준조사선량률 $\dot{X}_c$은 Exradin A-2공동 전리함을 일본 ETL로부터 교정하여 X-선 선질을 ETL 교정선질과 같도록 반가층을 결정한 후에 측정되었다.

한편, 흡수선량 및 깊이—선량 백분율 측정의 정확도를 검증하기 위해 phantom 속 깊이 5 cm되는 교정점에서 물속흡수선량률, $\dot{D}_w$을 N_k로부터 산출한 값과 Burlin의 일반화된 공동이론을 이용하여 계산한 값을 비교해 보았으며, N_k로부터 결정된 깊이—선량 백분율 P(%)을 BJR Suppl. 로부터 구한 값과 비교해 본 결과는 좋은 일치를 보였다.